catalysts

MDPI

Article

Increased Aromatics Formation by the Use of High-Density Polyethylene on the Catalytic Pyrolysis of Mandarin Peel over HY and HZSM-5

Young-Kwon Park [1], Muhammad Zain Siddiqui [2], Yejin Kang [2], Atsushi Watanabe [3], Hyung Won Lee [1], Sang Jae Jeong [2], Seungdo Kim [2] and Young-Min Kim [2,*]

1 School of Environmental engineering, University of Seoul, Seoul 130-743, Korea; catalica@uos.ac.kr (Y.-K.P.); adexhw@nate.com (H.W.L.)
2 Department of Environmental Sciences and Biotechnology, Hallym University, Chuncheon 24252, Korea; mohammedxainsiddiqui@gmail.com (M.Z.S.); cjswrokdv@naver.com (Y.K.); gabriel4627@gmail.com (S.J.J.); sdkim@hallym.ac.kr (S.K.)
3 Frontier Laboratories Ltd., 4-16-20, Saikon, Koriyama, Fukushima 963-8862, Japan; ichi@frontier-lab.com
* Correspondence: analyst@hallym.ac.kr; Tel.: +82-33-248-3324

Received: 27 November 2018; Accepted: 10 December 2018; Published: 12 December 2018

Abstract: High-density polyethylene (HDPE) was co-fed into the catalytic pyrolysis (CP) of mandarin peel (MP) over different microporous catalysts, HY and HZSM-5, with different pore and acid properties. Although the non-catalytic decomposition temperature of MP was not changed during catalytic thermogravimetric analysis over both catalysts, that of HDPE was reduced from 465 °C to 379 °C over HY and to 393 °C over HZSM-5 because of their catalytic effects. When HDPE was co-pyrolyzed with MP over the catalysts, the catalytic decomposition temperatures of HDPE were increased to 402 °C over HY and 408 °C over HZSM-5. The pyrolyzer-gas chromatography/mass spectrometry results showed that the main pyrolyzates of MP and HDPE, which comprised a large amount of oxygenates and aliphatic hydrocarbons with a wide carbon range, were converted efficiently to aromatics using HY and HZSM-5. Although HY can provide easier diffusion of the reactants to the catalyst pore and a larger amount of acid sites than HZSM-5, the CP of MP, HDPE, and their mixture over HZSM-5 revealed higher efficiency on aromatics formation than those over HY due to the strong acidity and more appropriate shape selectivity of HZSM-5. The production of aromatics from the catalytic co-pyrolysis of MP and HDPE was larger than the theoretical amounts, suggesting the synergistic effect of HDPE co-feeding for the increased formation of aromatics during the CP of MP.

Keywords: mandarin peel; high density polyethylene; HZSM-5; aromatic hydrocarbons

1. Introduction

Biomass pyrolysis is considered as a promising technology because biomass can be converted to bio-oil easily at medium high temperatures between 400 and 600 °C under a non-oxygen atmosphere [1]. The increased use of biochar produced as a byproduct of biomass pyrolysis is also elevating the value of biomass pyrolysis [2]. The impending crisis related to fossil fuel depletion, environmental contamination, and climate change, have also emphasized the value of biomass as the feedstock for thermal conversion technology to produce energy or chemical feedstock [3].

Mandarin is a seedless citrus fruit that is harvested widely in the world because of its sweet taste and easy peeling property [4]. Owing to the large content of peel in mandarin fruit, the amount of waste mandarin peel (MP) has also increased dramatically and most of them were landfilled or dumped into the ocean [5]. Recently, the Korean government prohibited the dumping of waste MP into

the ocean for the ocean's environmental preservation and the proper treatment of waste MP, which has become an urgent issue in the mandarin production area, such as Jeju Island in Korea [6]. The thermal treatment of MP has potential because of its high volatile content and heating value [7].

Several studies examined the pyrolysis of citrus peel [8–10]. Kim et al. [10] performed the kinetic and product analysis for the pyrolysis of MP. They reported that MP was converted to oxygenated compounds, such as alcohols, furans, ketones, phenols, fatty acids, limonene, and vitamins, mainly between 150 and 600 °C. Although various types of oxygenates can be produced from the pyrolysis of MP, pyrolysis oil is unsuitable for use as a fuel or chemical feedstock because of its high acidity and instability similar to the pyrolysis oil of other woody biomass.

To produce more stable and value-added biomass pyrolysis oil, catalytic fast pyrolysis (CFP) has been attempted on various kinds of biomass, such as wood, algae, and rice husk. On the other hand, the low yield of target aromatics products in the CFP oil of biomass and rapid catalyst deactivation limit the commercialization of the CFP process [11]. Kim et al. [12] also investigated the CFP of citrus peel. They found that citrus peel can produce larger amounts of aromatics than wood during the CFP over HZSM-5 due to the presence of pectin and a smaller lignin content in citrus peel. Nevertheless, the amount of aromatics was still low and an additional process is required to increase the yield of aromatics.

One of the possible ways to increase the yield of aromatics from biomass is the co-feeding of hydrogen-sufficient feedstock to the CFP process of biomass. Many researchers used plastics as the co-feeding feedstock to the CFP of biomass to increase the aromatics production efficiency [13]. Xue et al. [14] increased aromatics formation via the catalytic co-pyrolysis (CCP) of cellulose and polyethylene (PE). They explained that a more effective hydrocarbon pool formation and interactions between the CFP intermediates of the biomass and PE can increase aromatics production capability. Kim et al. [15] also indicated that the co-feeding of PE to the CFP of biomass can allow a more efficient reaction not only for the formation of aromatics, but also for decreasing coke formation. On the other hand, although the CCP of citrus peels and plastics can be considered as a potential for increasing the final yield of aromatics, there are no reports of this process being applied to the CCP of MP.

In this study, the CFP of MP, high density PE (HDPE), and their mixture over HY and HZSM-5, having different pore and acidity, was investigated using a thermogravimetric (TG) analyzer and pyrolyzer-gas chromatography/mass spectrometry (Py-GC/MS) to know the effect of catalysts and co-feeding of MP and HDPE on aromatics production. For TG analysis, MP, HDPE, or their mixture blended with HZSM-5 or HY was heated under a non-oxygen atmosphere at 5 °C/min. Py-GC/MS analysis for the same samples was performed at 600 °C to understand the effect of the CCP by comparing the yields of aromatics produced from the catalytic pyrolysis of MP, HDPE, and their mixture.

2. Results and Discussion

2.1. Thermogravimetric (TG) Analysis

Figure 1 shows the non-catalytic TG and derivative TG (DTG) curves of MP, HDPE, and their mixture at 5 °C/min. The initial (T_{onset}), maximum (T_{max}), and final (T_{offset}) temperature of each decomposition region (*M*1, *M*2, and *H*) on the thermal and catalytic DTG curves of MP, HDPE, and their mixture were also shown in Table 1. MP and HDPE were decomposed at different temperature regions. MP was decomposed over a wide temperature range between 160 and 354 °C (*M*1 and *M*2). The decomposition peaks (*M*1 and *M*2) on the DTG curves of MP can be assigned as the decomposition of pectin and cellulose, the main lignocellulosic components of citrus peels [7]. HDPE was decomposed at a narrow temperature range between 397 and 495 °C (*H*). The decomposition of MP/HDPE mixture was initiated at 161 °C and finalized at 495 °C of MP and HDPE. The peak heights for the decomposition of MP and HDPE on the DTG curve of the MP/HDPE mixture were approximately half of the heights for the peaks on the DTG curve of MP and that of HDPE because the same amount of MP and HDPE

were mixed (MP/HDPE: 1/1). The yield of solid residue for the TG analysis of MP/HDPE mixture (8.5%) was also about half of the summed solid yield of MP (17.4%) and HDPE (0.1%). The T_{max}s of MP, 204 °C (*M*1) and 354 °C (*M*2), and that of HDPE, 465 °C (H), were also similar with those, 205 °C (*M*1), 355 °C (*M*1), and 464 °C (*M*1) obtained from their co-pyrolysis. This suggests that the decomposition temperatures of MP and HDPE were not changed by their co-feeding to the non-catalytic TG analysis.

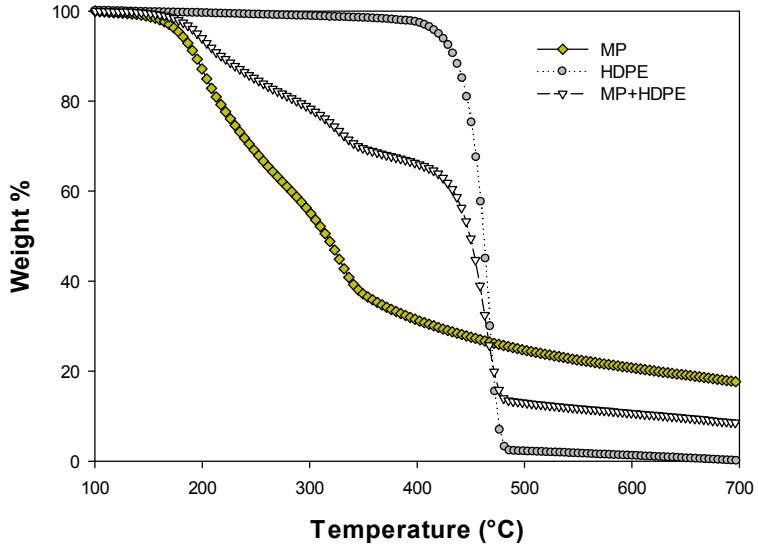

(**a**) Thermogravimetric (TG) analysis.

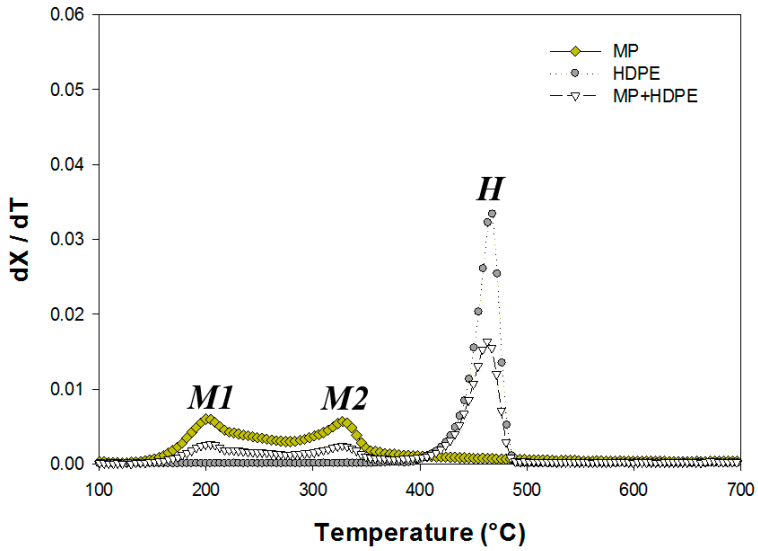

(**b**) Derivative thermogravimetric (DTG) analysis.

Figure 1. Non-catalytic TG and DTG curves of mandarin peel (MP), high-density polyethylene (HDPE), and their mixture at 5 °C/min.

Table 1. Thermal and catalytic degradation temperature properties of MP, HDPE, and their mixture at 5 °C/min (Unit: °C).

		*M*1		*M*2		*H*		
Sample	**Catalyst**	T_{onset}	T_{max}	T_{max}	T_{offset}	T_{onset}	T_{max}	T_{offset}
MP	No catalyst	160	204	328	354	-	-	-
HDPE	No catalyst	-	-	-	-	397	465	495
MP + HDPE	No catalyst	161	205	329	355	395	464	495
MP	HY	163	205	329	355	-	-	-
MP	HZSM-5	162	204	328	354	-	-	-
HDPE	HY	-	-	-	-	327	379	406
HDPE	HZSM-5	-	-	-	-	363	393	416
MP + HDPE	HY	160	204	328	345	350	402	459
MP + HDPE	HZSM-5	161	205	329	346	351	408	460

Figure 2 shows the thermal and catalytic DTG curves of MP, HDPE, and their mixture over HY and HZSM-5. The catalytic DTG curves of MP over both HY and HZSM-5 were not so different with its non-catalytic TG curve. T_{max}s on the catalytic DTG curves of MP over each catalyst, 205 °C (*M*1) and 329 °C (*M*2) over HY and 204 °C (*M*1) and 328 °C (*M*2) over HZSM-5, were not largely different from those obtained from the non-catalytic TG analysis of MP, 204 °C (*M*1) and 328 °C (*M*2). Low temperature differences (<2 °C) between the catalytic and non-catalytic DTG curves of MP suggest a minor catalytic effect of both HY and HZSM-5 on the change in the decomposition temperature of MP. Rezaei et al. [15] also found the unchanged decomposition temperature of biomass during the catalytic TG analysis of yellow poplar over different mesoporous catalysts. They explained the large molecular size of biomass derived compounds as the main factor limiting their diffusion to the catalyst pore.

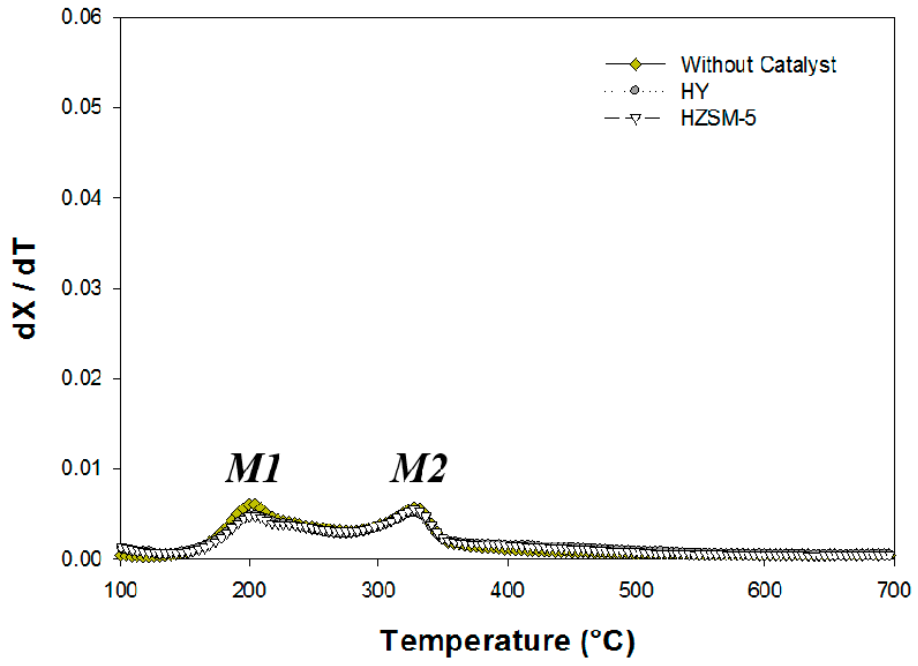

(**a**) MP

Figure 2. *Cont.*

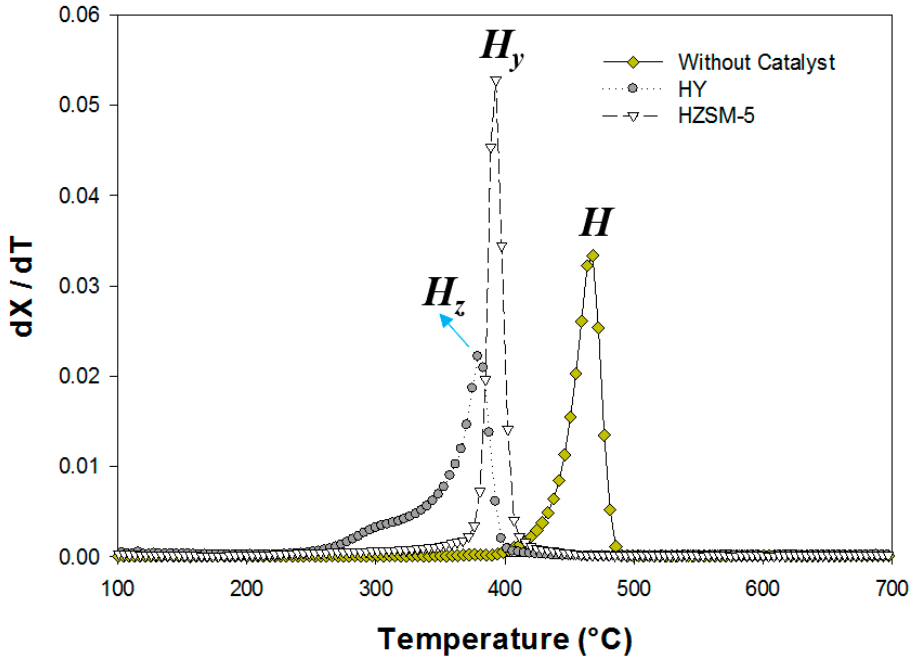

(**b**) HDPE

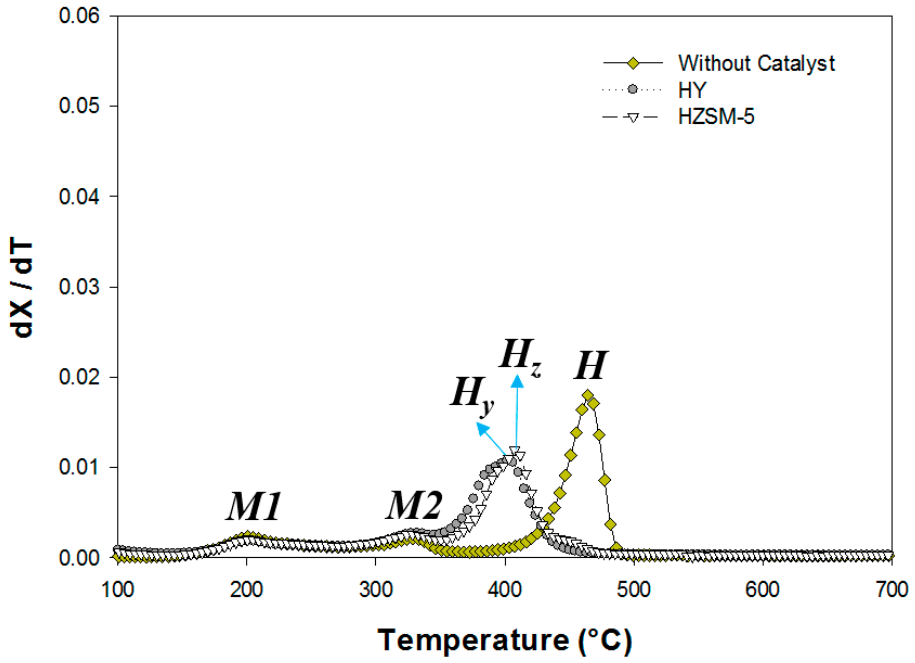

(**c**) MP + HDPE

Figure 2. Thermal and catalytic DTG curves of MP, HDPE and their mixture over HY and HZSM-5 at 5 °C/min.

Meanwhile, the decomposition temperatures of HDPE were lowered largely by the use of the catalysts, from 465 °C to 379 °C over HY and to 393 °C over HZSM-5 as shown in Figure 2b. This suggests that the acid catalysts reduced the decomposition temperature of HDPE due to the

smaller kinetic diameter of HDPE molecules than the catalyst pore size and the degradation efficiency of the catalysts is differentiated depending on the catalyst properties [16]. The stronger catalytic effect of HY lowering the HDPE decomposition temperature more than HZSM-5 can be explained by its larger number of acid sites (Figure 3), providing higher cracking efficiency and a larger pore size (Table 2), allowing a higher diffusion efficiency of reactants.

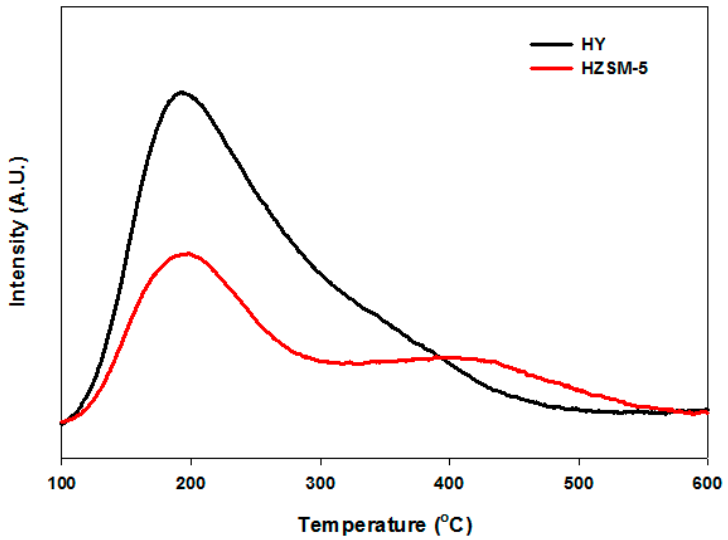

Figure 3. The temperature programmed desorption of ammonia (NH_3-TPD) curves of HY and HZSM-5 used in this study.

Table 2. Brunauer, Emmett and Teller (BET) surface area and pore size of HY and HZSM-5 used in this study.

Catalyst	SiO_2/Al_2O_3	S_{BET} (m^2/g)	Pore Size (nm)
HY	5.1	730	0.74 × 0.74
HZSM-5	23	382	0.51 × 0.55 (100) 0.53 × 0.56 (010)

The decomposition temperatures of MP during the catalytic co-TG analysis of a MP/HDPE mixture, Figure 2c, were similar to those observed on the non-catalytic DTG curves of MP shown in Figure 1. The HDPE decomposition temperatures on the catalytic DTG curves of the MP/HDPE mixtures, 402 °C (H_y) over HY and 408 °C (H_z) over HZSM-5, were higher than those on the catalytic DTG curves of HDPE, 379 °C over HY and 393 °C over HZSM-5. This indicates that the catalytic effects of HY and HZSM-5 were reduced by catalyst deactivation caused by the catalytic pyrolysis (CP) of MP at lower temperatures than for HDPE decomposition. A similar phenomenon was also observed during the catalytic TGA of a mixture of other biomass and HDPE. Kim et al. [17] reported that the HDPE decomposition temperature during its catalytic TGA was increased when cellulose was co-pyrolyzed with HDPE because the coke accumulated by the CP of cellulose deactivates the catalyst and reduces the HDPE decomposition efficiency of the catalyst.

2.2. Pyrolyzer-Gas Chromatography/Mass Spectrometry (Py-GC/MS) Analysis

(1) Mandarin Peel (MP)

Figure 4 presents Py-GC/MS chromatograms for the non-catalytic fast pyrolysis (NCFP) and CFP of MP over HY and HZSM-5 at 600 °C. The NCFP of MP produced many types of oxygenates, such as methanol, acetic acid, ketones, furans, phenols, and levoglucosan. Kim et al. [18] compared the pyrolysis of citrus peels and wood and reported that the relative contents of methanol and furans in the pyrolysis oil of citrus peel were higher than those of wood pyrolysis oil. They explained that the large

amount of methanol is formed by the demethoxylation of pectin occupying the largest portion among the lignocellulosic components of MP. Methanol and furfural were formed as the main pyrolyzates of pectin via rapid pyrolysis [19,20]. Acetic acid and furans are the typical hemicellulose pyrolysis products and levoglucosan is produced by the primary decomposition of cellulose [21]. Kim et al. [18] also reported that the NCFP of citrus peel produced smaller amounts of phenols than that of wood due to the smaller lignin content in citrus peel. This is more advantageous in aromatics production because lignin is converted more easily to char and coke than hemicellulose and cellulose during the CFP of biomass [12].

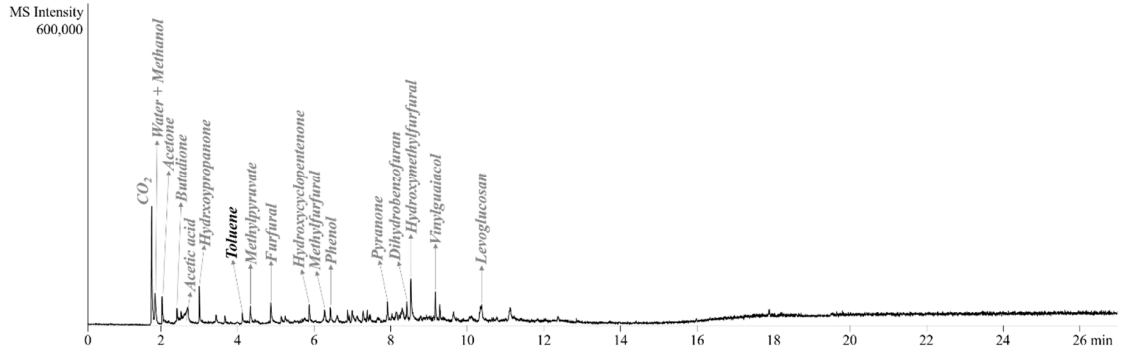

(**a**) No catalyst.

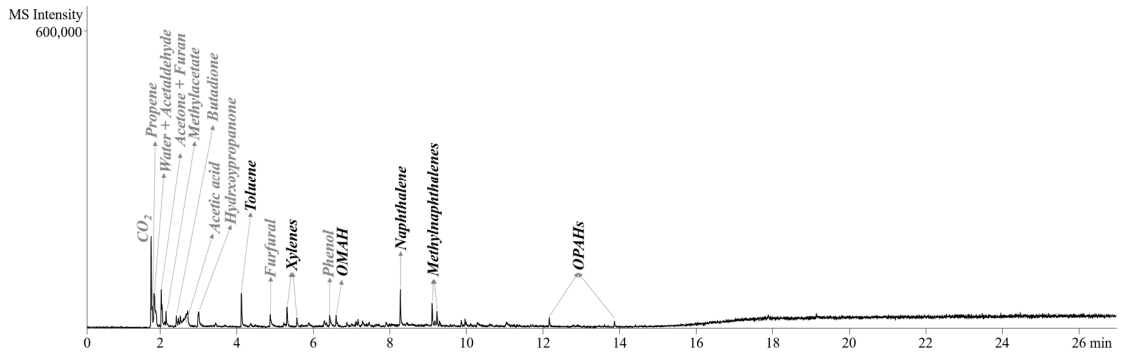

(**b**) Over HY.

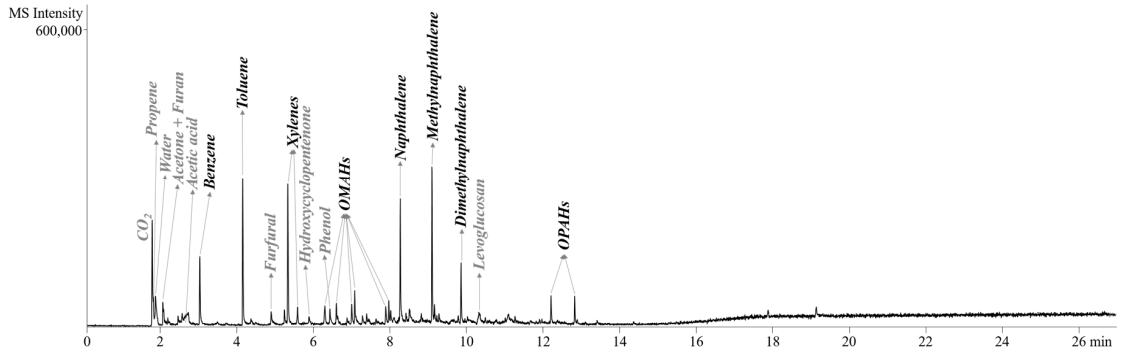

(**c**) HZSM-5.

Figure 4. Mass spectrometry (MS) chromatograms obtained from the non-catalytic fast pyrolysis (NCFP) and CFP of MP over HY and HZSM-5 at 600 °C. (OMAHs: other mono aromatic hydrocarbons, OPAHs: Other poly aromatic hydrocarbons).

Compared to the NCFP of MP, the CFP of MP over both HY and HZSM-5 produced smaller amount of oxygenates larger amounts of aromatics, suggesting the efficient conversion of oxygenates to aromatics via the hydrocarbon pool [22] and phenolic pool mechanism [23] during the CFP of biomass

over the catalysts. During the CFP of biomass, the main pyrolyzates of biomass are deoxygenated by the dehydration, dehydroxylation, decarbonylation, and decarboxylation and converted to light olefins together with the emission of water, CO, and CO_2 [18]. These light olefins can form the effective hydrocarbon pool and be converted to aromatics via a Diels–Alder reaction inside the pore of catalysts [24]. Phenolic pool mechanism is explained as the main mechanism on the formation of aromatics via the CFP of lignin. During the CFP of lignin, the phenolic intermediates form the phenolic pool inside the catalyst pore and are converted to aromatic hydrocarbons via dealkoxylation and dealkylation, or coke by their oligomerization [25].

In our results, the peak intensities for phenol and levoglucosan on the chromatogram obtained from the CFP of MP over HY were smaller than those over HZSM-5, Figure 4b, suggesting the higher deoxygenation efficiency of HY. The higher deoxygenation efficiency of HY can be explained by its larger pore size (Table 2) and larger amount of acid sites (Figure 3). Although HY showed a higher deoxygenation efficiency than HZSM-5, the CFP of MP over HZSM-5 revealed the much higher peak intensities for aromatics, indicating the higher efficiency on the production of aromatic hydrocarbons of HZSM-5 than HY during the CFP of MP. The proper pore size of HZSM-5 allowing the more appropriate shape selectivity for aromatics formation than HY (Table 2, [12]) and its stronger acidity (Figure 3) can be suggested as its higher aromatics production efficiency. Kim et al. [12] compared aromatics formation efficiency during the sequential CFP of citrus peel over HZSM-5 and HY. Although they used the different HY having different acidity to that used in this study, they also found that HY produced the smaller amount of aromatics and larger amount of coke during the CFP of MP than HZSM-5. When the pore size of the catalyst was larger than the size required for the production of aromatics, the amount of coke could be increased because of the additional oligomerization of reaction intermediates inside the catalyst [26].

(2) ***High-Density Polyethylene (HDPE)***

HDPE pyrolysis mainly produced three types of aliphatic hydrocarbons, such as alkadiene, alkene, and alkane, in a wide carbon range up to C_{40}, Figure 5a [14]. The random chain scission of HDPE via a radical mechanism is suggested as the main reaction pathways for the formation of these aliphatic hydrocarbons [27]. Although many products were produced from the NCFP of HDPE, they are difficult to be used as fuels because of the wide carbon range in HDPE pyrolysis oil. Figure 5b,c show the PY-GC/MS chromatograms for the CFP of HDPE over HY and HZSM-5. Compared to the CFP of MP shown in Figure 4b,c, the CFP of HDPE over both catalysts produced much larger amounts of aromatics and light hydrocarbons owing to its higher carbon and hydrogen contents than MP [17]. Between the two catalysts, HZSM-5 showed the higher efficiency on aromatics production than HY because of its higher shape selectivity toward mono-aromatics than HY. HZSM-5 mainly produced BTEXs (benzene, toluene, ethylbenzene, and xylenes) and naphthalenes, such as naphthalene, methylnaphthalenes, and dimethylnaphthalenes, during the CCP of HDPE. Meanwhile, HY revealed the higher selectivity to other mono aromatic hydrocarbons (OMAHs), and alkyl naphthalenes. The formation of large amounts of branched aromatic hydrocarbons over HY is possible due to the its higher surface area and larger cavities in HY structure (Table 2, [28]). As observed on the chromatograms for the CFP of HDPE, the peak intensities for light olefins (C_2~C_5) were much higher than those of aromatic hydrocarbons. This suggests that these light olefins can be converted to aromatic hydrocarbons additionally by increasing the amount of catalyst because the added catalyst can enhance the additional aromatization reaction [29]. These light olefins also can be used as the hydrogen donor to the oxygenated CFP intermediates, such as furan, enhancing the synergistic formation of aromatics during the catalytic pyrolysis of biomass and HDPE [14].

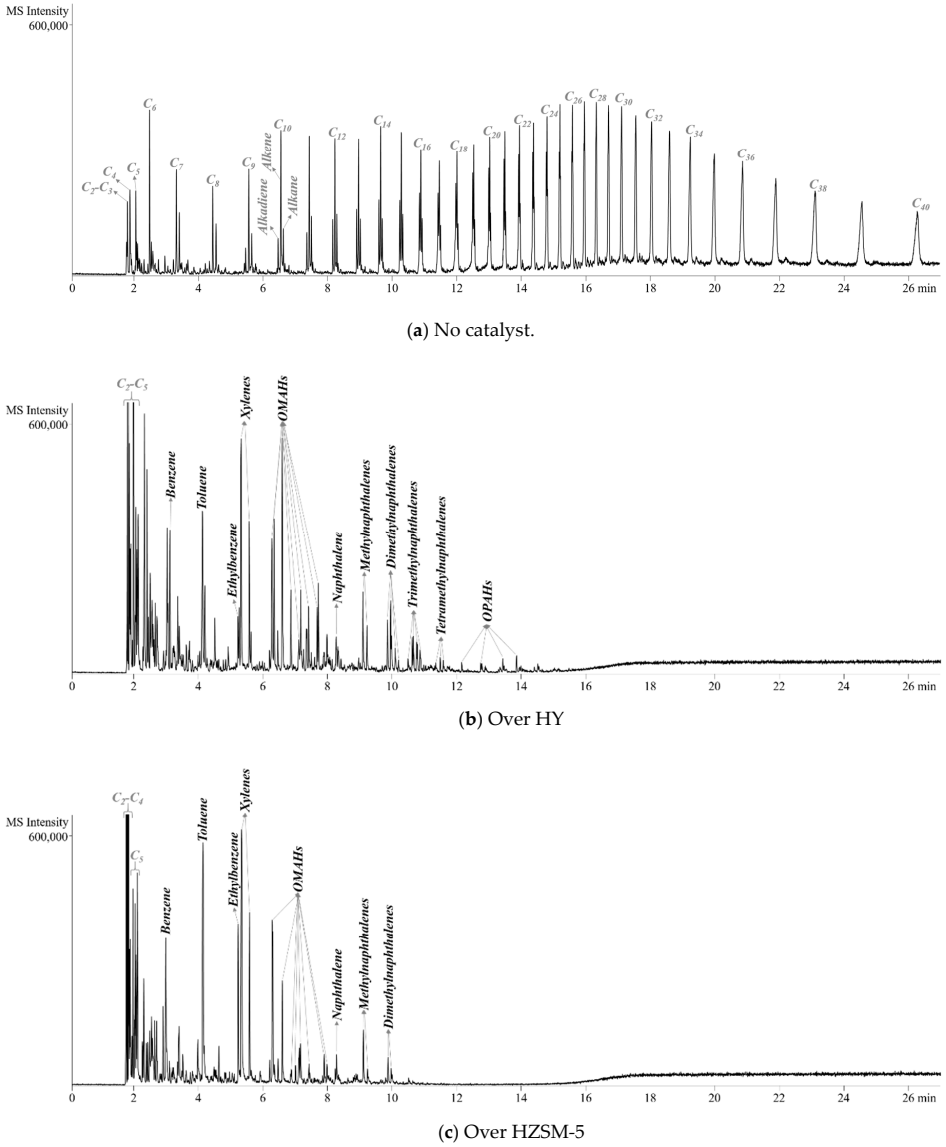

Figure 5. MS chromatograms obtained from the NCFP and CFP of HDPE over HY and NZSM-5 at 600 °C.

(3) The Mixture of MP and HDPE

Figure 6 shows the Py-GC/MS chromatograms obtained from the non-catalytic co-fast pyrolysis (NCCFP) and catalytic co-fast pyrolysis (CCFP) of MP/HDPE mixture over HY and HZSM-5, respectively. The NCCFP of MP had the typical pyrolyzates of MP, many kinds of oxygenates shown in Figure 4a, and those of HDPE, alkadienes, alkenes, and alkanes in wide carbon range shown in Figure 5a. The peak intensities for these pyrolyzates of MP and HDPE shown on the chromatogram for the NCCFP of MP, Figure 6a, were about half of those shown in the NCCFP of MP/HDPE mixture, Figure 4a, and those of HDPE, Figure 5a, suggesting no interaction between the pyrolysis intermediates of MP and HDPE. The CCFP of MP and HDPE over HZSM-5 revealed the higher intensities for BTEXs and naphthalenes than that over HY. Meanwhile, HY produced larger amounts of OMAHs, such as tri- and tetramethyl benzenes and alkyl naphthalenes. Although their intensities were not higher, the chromatogram for the CCFP of MP/HDPE mixture over HZSM-5 had the peaks for the typical pyrolyzates of NCFP of HDPE, alkadienes, alkenes, and alkadienes in wide carbon range shown in Figure 5a. This can be explained by the limited diffusion of HDPE molecules by the MP derived char or coke, as expected during on the TG analysis for the catalytic TG analysis of MP/HDPE mixture.

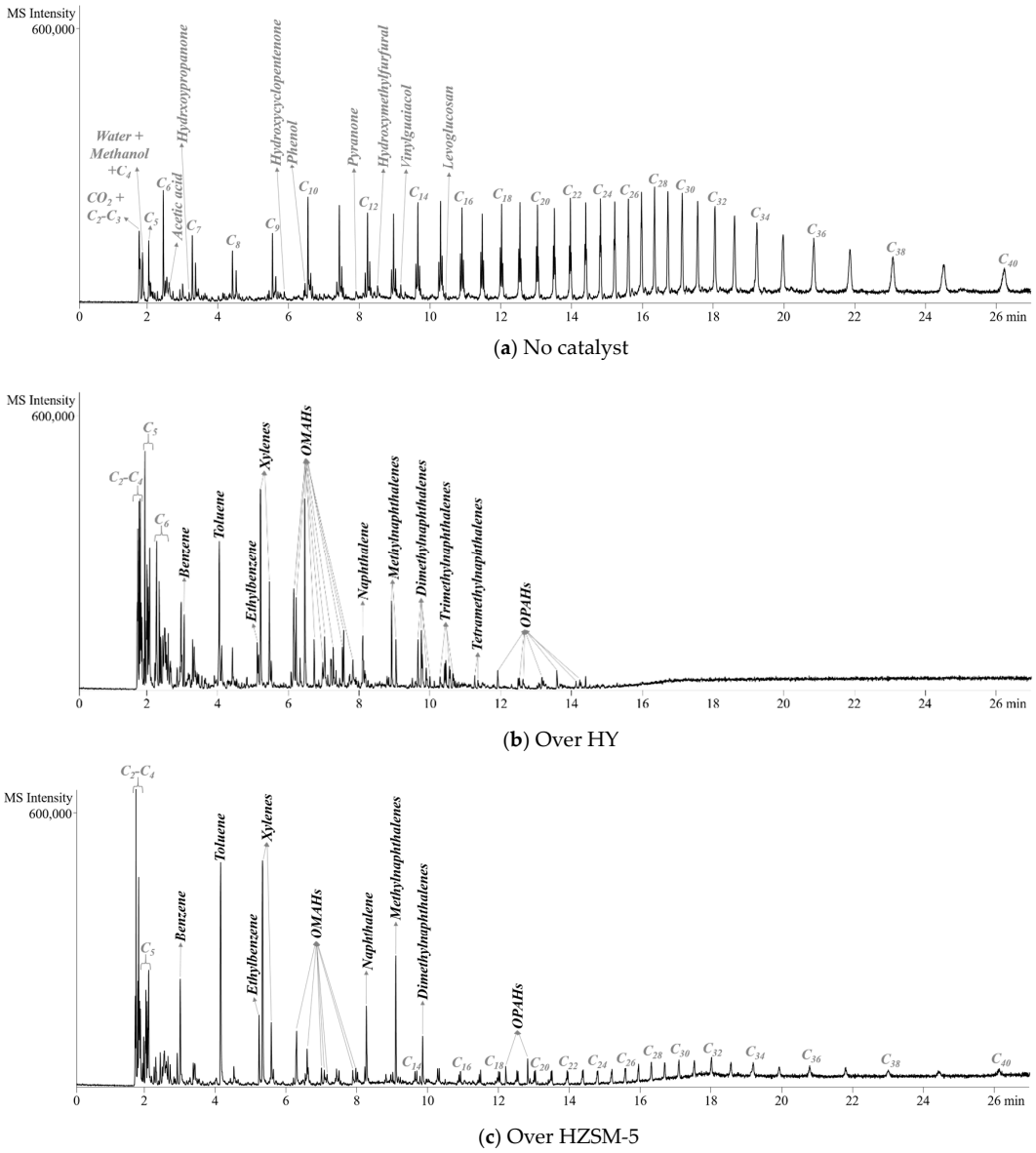

Figure 6. MS chromatograms obtained from the non-catalytic co-fast pyrolysis (NCCFP) and CCFP of MP/HDPE mixture over HY and HZSM-5 at 600 °C.

Theoretically, the peak intensities for the aromatics obtained from the CCFP of MP and HDPE, Figure 6b,c, should be half the summed intensities for those obtained from the individual CFP of MP, Figure 4b,c, and HDPE, Figure 5b,c, over the same catalyst because the same amounts of MP and HDPE were co-fed to their CCFP (MP/HDPE: 1/1). However, the peak intensities for aromatic hydrocarbons in Figure 6 were higher than the average values for those obtained from the CFP of MP and HDPE. In addition, the peaks for oxygenates, such as ketones, furans, and phenols, shown in Figure 4b,c were almost absent on the chromatogram for the CCFP of MP/HDPE mixture, Figure 6b,c. This suggests that there are some interactions between the CFP reaction intermediates of MP and HDPE, also converting oxygenates to aromatic hydrocarbons during CCFP over HY and HZSM-5.

Figure 7 shows the synergistic formation of aromatics on the CCFP of MP and HDPE over HY and HZSM-5, respectively. The detailed yields of aromatics obtained from the catalytic pyrolysis of MP, HDPE, and their mixture were also shown in Table S1 (Supplementary Information). The experimental yields (wt.%) of aromatics obtained from the CCFP of MP and HDPE, 5.06% over HY and 6.04% over HZSM-5, were higher than their theoretical yields, 4.20% over HY and 5.54% over HZSM-5, calculated

from those obtained from the individual CFP of MP and HDPE. This definitely indicates additional aromatics formation by applying the co-feeding of HDPE to the CFP of MP over both catalysts. Between HY and HZMS-5, HZSM-5 produced aromatics more efficiently than HY during the CCFP of MP and HDPE, suggesting additional interactions between the CFP reaction intermediates of MP and HDPE, increasing aromatics formation. The additional aromatics production can be explained by the effective Diels–Alder reaction between the residual oxygenates, such as methanol and furfural, formed from the CFP of MP, and light olefins formed from the CFP of HDPE over both catalysts. Aromatics formation via an effective Diels–Alder reaction between furans and light olefins has been reported as the main reaction pathway for the additional aromatics formation during the CCFP of biomass and HDPE over acid catalysts [30]. The relatively large amounts of methanol in MP pyrolyzates also can be efficiently converted to light olefins and aromatics over acid catalysts [31,32]. The light olefins from the catalytic reaction of methanol can reinforce the hydrocarbon pool inside the catalyst pores, leading to the additional formation of aromatic hydrocarbons. Therefore, several researchers also co-fed methanol during the CFP of biomass. Asadieraghi et al. [33] reported that an additional amount of aromatic hydrocarbons can be achieved by co-feeding methanol to the CFP of palm kernel shell. They explained that the methanol can be converted to dimethyl ether via acid catalyzed dehydration over HZSM-5 and forms a hydrocarbon pool that can enhance the formation of aromatics.

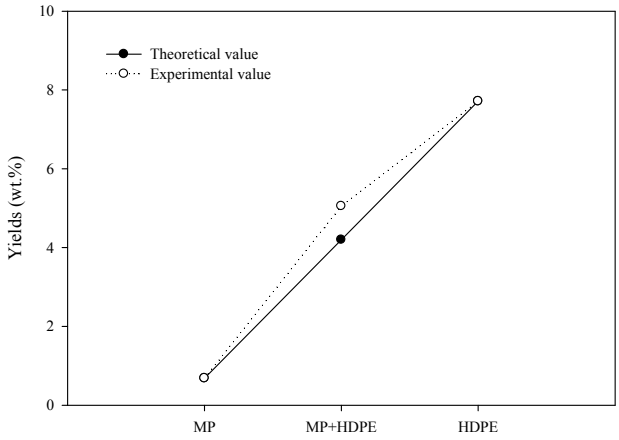

(**a**) HY

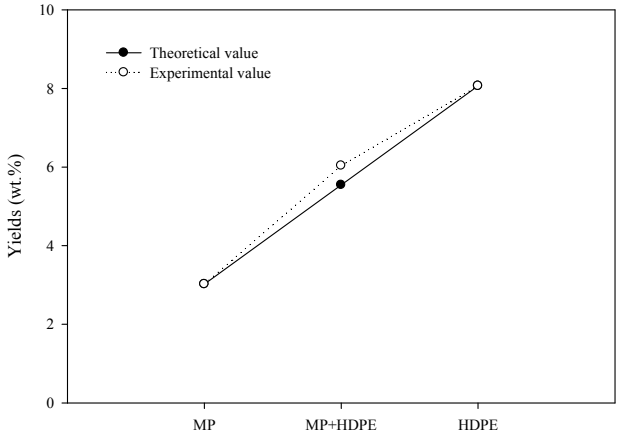

(**b**) HZSM-5

Figure 7. Theoretical and experimental yields (wt.%) of aromatics obtained from the CCFP of MP and HDPE over HY and HZSM-5.

3. Materials and Methods

3.1. MP and HDPE

MP was obtained by peeling off the mandarin fruit harvested from Jeju island (South Korea). HDPE was purchased from LG Chemical (Yeosu, South Korea). MP was dried at ambient temperature during 4 days to eliminate the moisture. Dried MP and HDPE were cryo-milled to make particles smaller than 200 μm and dried at 60 °C for 1 day. The physico-chemical properties of MP and HDPE were listed in Table S2. HDPE had a larger content of volatiles than MP and only C and H as the main elements. This suggests that HDPE has a much higher effective carbon to hydrogen ratio (C/H_{eff}) than MP, suggesting its potential use as a hydrogen donor to the CFP of MP [18,30].

3.2. Catalyst

Two kinds of zeolites having different SiO_2/Al_2O_3, HY (SiO_2/Al_2O_3: 5.1) and HZSM-5 (SiO_2/Al_2O_3: 23), were purchased from Zeolyst International (Conshohocken, PA, USA). The physico-chemical properties of the catalysts are shown in Table 1. NH_3-TPD analysis was performed to know the catalyst acidity according to the procedure reported in previous literature [12]. NH_3-TPD curves of HY and HZSM-5 (Figure 2) indicated that HY had the larger acid amount (1.96 mmol NH_3/g) than HZSM-5 (1.40 mmol NH_3/g). However, HZSM-5 had the stronger acidity than HY. Both catalysts were calcined at 550 °C in air and kept in a desiccator to avoid water penetration before all experiments.

3.3. TG Analysis

A 4 mg sample of MP, HDPE, or their mixture (MP/HDPE: 1/1) was degraded non-isothermally in a TG analyzer (Pyris 1, Perkin Elmer, Waltham, MA, USA) from ambient temperature to 800 °C at 5 °C/min under a nitrogen atmosphere (50 mL/min). In the case of CP or CCP reactions, 4 mg of catalyst (HY or HZSM-5) was mixed with the same amount of MP, HDPE, and their mixture (Catalyst/Sample: 1/1).

3.4. Py-GC/MS Analysis

A conventional pyrolyzer (Py-3030D, Frontier Laboratories Ltd., Koriyama, Japan) connected directly to a GC/MS system (7890A/5975C inert, Agilent Technology, CA, USA), Figure S1, was used for the rapid NCFP and CFP of MP, HDPE, and their mixtures over each catalyst. For NCFP, 1 mg of MP, HDPE, or their mixture (MP/HDPE: 1/1) was injected to the preheated pyrolysis heater (600 °C) for their fast pyrolysis. The pyrolysis product vapor was transferred to the GC separation column (UA-5, 30 m length × 0.25 mm inner diameter × 0.25 μm film thickness, Frontier Laboratories Ltd., Koriyama, Japan) via GC inlet (320 °C, split 200:1) and cryo-focused using liquid nitrogen (−195 °C) at the front part of the column. After the cryo-focusing time (3 min), the products were separated by a GC oven temperature program, from 40 °C (3 min) to 320 °C (5 min) at 12 °C/min, and a constant column flow (He, 1 mL/min) and detected using a single quadrupole MS (Scan range: m/z 15–600, Scan speed: 3.69 scans/sec). For the CFP or CCFP, 1 mg of catalyst blended physically with 1 mg of sample, MP, HDPE, or their mixture, was pyrolyzed under the same condition used for NCFP. The separated products were identified using a MS library (F-Search, Frontier Laboratories Ltd., Koriyama, Japan) and the MS peaks of the products were integrated. The yields of aromatic hydrocarbons were calculated by the external standard calibration method using chemical standard mixtures. All Py-GC/MS experiments were repeated more than two times and the relative standard deviation (RSD) values for the peak areas of target aromatic hydrocarbons were less than 5.0%.

4. Conclusions

The co-feeding of HDPE to the CP of MP over HY and HZSM-5 was evaluated by a TG analyzer and Py-GC/MS. Although the catalytic TG analysis of a HDPE and MP/HDPE mixture over HY

resulted in a lower HDPE decomposition temperature than those over HZSM-5 owing to its larger number of acid sites and larger pore size, a much larger quantity of aromatics was obtained when HZSM-5 was used in the CFP of HDPE and MP/HDPE mixture instead of HY owing to its higher shape selectivity toward aromatics and strong acid sites. The CCFP of MP and HDPE achieved additional aromatics production due to the hydrogen donating efficiency of HDPE and the more effective Diels–Alder reaction between the CFP intermediates of MP and HDPE over both HY and HZSM-5.

Supplementary Materials: The following are available online at http://www.mdpi.com/2073-4344/8/12/656/s1, Table S1: The yields of aromatics obtained from the catalytic pyrolysis of MP, HDPE, and their mixture over HY and HZSM-5 at 600 °C; Table S2: Physico-chemical properties of MP and HDPE; Figure S1: The Schematic diagram of Pyrolyzer-GC/MS.

Author Contributions: Conceptualization, Y.-K.P. and Y.-M.K.; Data curation, M.Z.S. and Y.K.; Formal analysis, A.W. and H.W.L.; Investigation, S.K. and S.J.; Methodology, A.W. and S.K.; Supervision, Y.-M.K.; Validation, S.K. and Y.-K.P.; Visualization, S.K.; Writing–original draft, Y.-K.P.; Writing–review and editing, Y.-M.K.

Funding: This research was supported by a grant (18IFIP-B113506-03) from the development of the plant program funded by the Ministry of Land, Infrastructure and Transport of the Korean government.

Conflicts of Interest: The authors declare no conflict of interest.

References

1. Kim, Y.M.; Park, S.; Kang, B.S.; Jae, J.; Rhee, G.H.; Jung, S.C.; Park, Y.K. Suppressed char agglomeration by rotary kiln reactor with alumina ball during the pyrolysis of kraft lignin. *J. Ind. Eng. Chem.* **2018**, *66*, 72–77. [CrossRef]
2. Lee, H.W.; Kim, Y.M.; Kim, S.; Ryu, C.; Park, S.H.; Park, Y.K. Review of the use of activated biochar for energy and environmental applications. *Carbon Lett.* **2018**, *26*, 1–10.
3. Lee, H.; Kim, Y.M.; Lee, I.G.; Jeon, J.K.; Jung, S.C.; Chung, J.D.; Choi, W.G.; Park, Y.K. Recent advances in the catalytic hydrodeoxygenation of bio-oil. *Korean J. Chem. Eng.* **2016**, *33*, 3299–3315. [CrossRef]
4. Goldenberg, L.; Yaniv, Y.; Porat, R.; Carmi, N. Mandarin fruit quality: A review. *J. Sci. Food Agric.* **2018**, *98*, 18–26. [CrossRef] [PubMed]
5. Choi, I.S.; Lee, Y.G.; Khanal, S.K.; Park, B.J.; Bae, H.J. A low-energy, cost-effective approach to fruit and citrus peel waste processing for bioethanol production. *Appl. Energy* **2015**, *140*, 65–74. [CrossRef]
6. Kim, J.W.; Park, S.H.; Jung, J.; Jeon, J.K.; Ko, C.H.; Jeong, K.E.; Park, Y.K. Catalytic pyrolysis of mandarin residue from the mandarin juice processing industry. *Bioresour. Technol.* **2013**, *136*, 431–436. [CrossRef] [PubMed]
7. Kim, Y.M.; Lee, H.W.; Lee, S.H.; Kim, S.S.; Park, S.H.; Jeon, J.K.; Kim, S.; Park, Y.K. Pyrolysis properties and kinetics of mandarin peel. *Korean J. Chem. Eng.* **2011**, *28*, 2012–2016. [CrossRef]
8. Lee, H.W.; Lee, H.; Cha, J.S.; Jeon, J.K.; Park, S.H.; Jung, S.C.; Kim, J.M.; Kim, S.C.; Park, Y.K. Catalytic pyrolysis of *Citrus unshiu* peel over mesoporous catalysts. *Sci. Adv. Mater.* **2017**, *9*, 1015–1019. [CrossRef]
9. Miranda, R.; Bustos-Martinez, D.; Blanco, C.S.; Villarreal, M.H.G.; Cantu, M.E.R. Pyrolysis of sweet orange (*Citrus sinensis*) dry peel. *J. Anal. Appl. Pyrolysis* **2009**, *86*, 245–251. [CrossRef]
10. Kim, Y.M.; Lee, H.W.; Kim, S.; Watanabe, C.; Park, Y.K. Non-isothermal pyrolysis of *Citrus unshiu* peel. *Bioenerg. Res.* **2015**, *8*, 431–439. [CrossRef]
11. Rahman, M.M.; Liu, R.; Cai, J. Catalytic fast pyrolysis of biomass over zeolites for high quality bio-oil-A review. *Fuel Process. Technol.* **2018**, *180*, 32–46. [CrossRef]
12. Kim, B.S.; Kim, Y.M.; Jae, J.; Watanabe, C.; Kim, S.; Jung, S.C.; Kim, S.C.; Park, Y.K. Pyrolysis and catalytic upgrading of *Citrus unshiu* peel. *Bioresour. Technol.* **2015**, *194*, 312–319. [CrossRef] [PubMed]
13. Zhang, X.; Lei, H.; Chen, S.; Wu, J. Catalytic co-pyrolysis of lignocellulosic biomass with polymer: A critical review. *Green Chem.* **2016**, *18*, 4145–4169. [CrossRef]
14. Xue, Y.; Kelkar, A.; Bai, X. Catalytic co-pyrolysis of biomass and polyethylene in a tandem micropyrolyzer. *Fuel* **2016**, *166*, 227–236. [CrossRef]
15. Rezaei, P.S.; Oh, D.; Hong, Y.; Kim, Y.M.; Jae, J.; Jung, S.C.; Jeon, J.K.; Park, Y.K. In-situ catalytic co-pyrolysis of yellow poplar and high-density polyethylene over mesoporous catalysts. *Energy Convers. Manag.* **2017**, *151*, 116–122. [CrossRef]

16. Kim, Y.M.; Lee, H.W.; Jae, J.; Jung, K.B.; Jung, S.C.; Watanabe, A.; Park, Y.K. Catalytic co-pyrolysis of biomass carbohydrates with LLDPE over Al-SBA-15 and mesoporous ZSM-5. *Catal. Today* **2017**, *298*, 46–52. [CrossRef]
17. Kim, B.S.; Kim, Y.M.; Lee, H.W.; Jae, J.; Kim, D.H.; Jung, S.C.; Watanabe, C.; Park, Y.K. Catalytic copyrolysis of cellulose and thermoplastics over HZSM-5 and HY. ACS Sustain. *Chem. Eng.* **2016**, *4*, 1354–1363.
18. Kim, Y.M.; Jae, J.; Lee, H.W.; Han, T.U.; Lee, H.; Park, S.H.; Kim, S.; Watanabe, C.; Park, Y.K. Ex-situ catalytic pyrolysis of citrus fruit peels over mesoporous MFI and Al-MCM-41. *Energy Convers. Manag.* **2016**, *125*, 277–289. [CrossRef]
19. Aburto, J.; Moran, M.; Galano, A.; Torres-Garcia, E. Non-isothermal pyrolysis of pectin: A thermochemical and kinetic approach. *J. Anal. Appl. Pyrolysis* **2015**, *112*, 94–104. [CrossRef]
20. Alvarez, J.; Hooshdaran, B.; Cortazar, M.; Amutio, M.; Lopez, G.; Freire, F.B.; Haghshenasfard, M.; Hosseini, S.H.; Olazar, M. Valorization of citrus wastes by fast pyrolysis in a conical spouted bed reactor. *Fuel* **2018**, *224*, 111–120. [CrossRef]
21. Wang, K.; Kim, K.H.; Brown, R.C. Catalytic pyrolysis of individual components of lignocellulosic biomass. *Green Chem.* **2014**, *16*, 727–735. [CrossRef]
22. Liu, C.; Wang, H.; Karim, A.M.; Sun, J.; Wang, Y. Catalytic fast pyrolysis of lignocellulosic biomass. *Chem. Soc. Rev.* **2014**, *43*, 7594–7623. [CrossRef] [PubMed]
23. To, A.T.; Resasco, D.E. Role of a phenolic pool in the conversion of m-cresol to aromatics over HY and HZSM-5 zeolites. *Appl. Catal. A-Gen.* **2014**, *487*, 62–71. [CrossRef]
24. Jae, J.; Tompsett, G.A.; Foster, A.J.; Hammond, K.D.; Auerbach, S.M.; Lobo, R.F.; Huber, G.W. Investigation into the shape selectivity of zeolite catalysts for biomass conversion. *J. Catal.* **2011**, *279*, 257–268. [CrossRef]
25. Lee, H.W.; Kim, Y.M.; Jae, J.; Sung, B.H.; Jung, S.C.; Kim, S.C.; Jeon, J.K.; Park, Y.K. Catalytic pyrolysis of lignin using a two-stage fixed bed reactor comprised of in-situ natural zeolite and ex-situ HZSM-5. *J. Anal. Appl. Pyrolysis* **2016**, *122*, 282–288. [CrossRef]
26. Park, Y.K.; Lee, B.; Watanabe, A.; Lee, H.W.; Lee, J.Y.; Kim, S.; Han, T.U.; Kim, Y.M. Catalytic copyrolysis of cork oak and waste plastic film over HBeta. *Catalysts* **2018**, *8*, 318. [CrossRef]
27. Yan, G.; Jing, X.; Wen, H.; Xiang, S. Thermal cracking of virgin and waste plastics of PP and LDPE in a semibatch reactor under atmospheric pressure. *Energy Fuels* **2015**, *29*, 2289–2298. [CrossRef]
28. Aho, A.; Kumar, N.; Eränen, K.; Salmi, T.; Hupa, M.; Murzin, D.Y. Catalytic pyrolysis of woody biomass in a fluidized bed reactor: Influence of the zeolite structure. *Fuel* **2008**, *87*, 2493–2501. [CrossRef]
29. Carlson, T.R.; Tompsett, G.A.; Conner, W.C.; Huber, G.W. Aromatic production from catalytic fast pyrolysis of biomass-derived feedstocks. *Top. Catal.* **2009**, *52*, 241–252. [CrossRef]
30. Lee, H.W.; Kim, Y.M.; Lee, B.; Kim, S.; Jae, J.; Jung, S.C.; Kim, T.W.; Park, Y.K. Catalytic copyrolysis of torrefied cork oak and high density polyethylene over a mesoporous HY catalyst. *Catal. Today* **2018**, *307*, 301–307. [CrossRef]
31. Zhang, H.; Carlson, T.R.; Xiao, R.; Huber, G.W. Catalytic fast pyrolysis of wood and alcohol mixture in a fluidized bed reactor. *Green Chem.* **2012**, *14*, 98–110. [CrossRef]
32. Atutxa, A.; Aguado, R.; Gayubo, A.G.; Olazar, M.; Bilbao, J. Kinetic description of the catalytic pyrolysis of biomass in a conical spouted bed reactor. *Energy Fuels* **2005**, *19*, 765–774. [CrossRef]
33. Asadieraghi, M.; Daud, W.M.A.W. In-situ catalytic upgrading of biomass pyrolysis vapor: Co-feeding with methanol in a multi-zone fixed bed reactor. *Energy Convers. Manag.* **2015**, *92*, 448–458. [CrossRef]